







## Article

# Biomechanical Assessment of Cannulated Nails for the Treatment of Proximal Femur Fractures

Karel Frydryšek<sup>1,2</sup> , Tomáš Halo<sup>1,2,\*</sup> , Daniel Čepica<sup>1,2</sup>, Vojtěch Machalla<sup>1,2</sup>, Kateřina Šimečková<sup>1,2</sup> , Ondřej Skoupý<sup>1,2</sup>, Roman Madeja<sup>2,3</sup>, Miroslav Havlíček<sup>4</sup>, Kamila Dostálová<sup>5</sup>, Antonín Trefil<sup>1</sup> , Leopold Pleva<sup>2,3</sup>, Zuzana Murčinkova<sup>6</sup> , Pavel Krpec<sup>7</sup> and Josef Hlinka<sup>8</sup> 

- <sup>1</sup> Faculty of Mechanical Engineering, VSB—Technical University of Ostrava, 17. listopadu 15/2172, 70800 Ostrava-Poruba, Czech Republic; karel.frydrysek@vsb.cz (K.F.); daniel.cepica@vsb.cz (D.Č.); vojtech.machalla@vsb.cz (V.M.); katerina.simeckova@vsb.cz (K.Š.); ondrej.skoupy@vsb.cz (O.S.); Antonin.trefil@vsb.cz (A.T.)
- <sup>2</sup> Faculty of Medicine, University of Ostrava, Syllabova 19, 70300 Ostrava-Vitkovice, Czech Republic; roman.madeja@fno.cz (R.M.); leopold.pleva@fno.cz (L.P.)
- <sup>3</sup> Trauma Centre, University Hospital Ostrava, 17. listopadu 1790, 70852 Ostrava-Poruba, Czech Republic
- <sup>4</sup> Medin, a.s, Vlachovicka 619, 59231 Nové Město na Moravě, Czech Republic; miroslav.havlicek@medin.cz
- <sup>5</sup> Centre for Advanced Innovative Technologies, VSB—Technical University of Ostrava, 17. listopadu 15/2172, 70800 Ostrava-Poruba, Czech Republic; kamila.dostalova@vsb.cz
- <sup>6</sup> Department of Design and Monitoring of Technical Systems, Technical University of Košice, Letná 9, 04200 Košice, Slovakia; zuzana.murcinkova@tuke.sk
- <sup>7</sup> V-NASS, a.s., Halasova 2938/1a, 70300 Ostrava-Vitkovice, Czech Republic; pavel.krpec@v-nass.cz
- <sup>8</sup> Faculty of Materials Science and Technology, VSB—Technical University of Ostrava, 17. listopadu 15/2172, 70800 Ostrava-Poruba, Czech Republic; josef.hlinka@vsb.cz
- \* Correspondence: tomas.halo@vsb.cz



**Citation:** Frydryšek, K.; Halo, T.; Čepica, D.; Machalla, V.; Šimečková, K.; Skoupý, O.; Madeja, R.; Havlíček, M.; Dostálová, K.; Trefil, A.; et al. Biomechanical Assessment of Cannulated Nails for the Treatment of Proximal Femur Fractures. *Appl. Sci.* **2022**, *12*, 7470. <https://doi.org/10.3390/app12157470>

Academic Editor: Gaetano Isola

Received: 15 April 2022

Accepted: 22 June 2022

Published: 25 July 2022

**Publisher's Note:** MDPI stays neutral with regard to jurisdictional claims in published maps and institutional affiliations.



**Copyright:** © 2022 by the authors. Licensee MDPI, Basel, Switzerland. This article is an open access article distributed under the terms and conditions of the Creative Commons Attribution (CC BY) license (<https://creativecommons.org/licenses/by/4.0/>).

**Abstract:** This article focuses on a type of surgical implant used in orthopaedics and traumatology—cannulated femoral nails. Femoral nails are used in medical treatment for purposes of osteosynthesis, i.e., when treating various types of complicated fractures, in this case fractures of the femur. The article investigates cases in which a nail has been implanted in the proximal part of the femur for a short time (with the fracture still not healed), compared with cases in which the bone has already healed. According to AO classification, examined fractures are described as AO 31B3 AO 32A3. The main focus is on strength-deformation analysis using the finite element method (FEM), which makes it possible to determine the behaviour of the femur-implant system. FEM analysis was used to compare 1.4441 steel nails made by two manufacturers, Medin (Czech Republic) and Tantum (Germany). Boundary conditions including external loading, prescribed supports and elastic foundation are defined. There were solved FEM analyses for five cases of healed femur and five cases of broken femur both including implants with prescribed colli-diaphyseal angles. The results of the analysis were used to assess stress-deformation states from the perspective of appropriateness for clinical treatment, biomechanical reliability and safety. All examined femoral nails are compared, safe and suitable for patient treatment.

**Keywords:** proximal femoral nailing; osteosynthesis; numerical simulation; traumatology; FEM analysis; biomechanics; short reconstructive nails

## 1. Introduction

In medical practice, nails are used to treat various types of limb fractures. Femoral nails are used to treat fractures of the proximal and distal femur. This article presents an analysis of nails used to treat proximal femoral fractures located in the vicinity of the pelvis. It also draws significance to the usage of short reconstructive nails in the treatment of specific proximal femur fractures. The examined nails are manufactured by Medin (Nové Město na Moravě, Czech Republic) and Tantum (Neumünster, Germany). It draws

on previous theoretical and practical studies concerning the proximal femur [1,2]. In the AO classification, the fractures in this region are *fractura mediocervicalis femoris* AO 31B3 and *fractura subtrochanterica femoris* AO 32A3 [3]. These are among the most frequent fractures of long bones, human trauma and they present the greatest risk to the elderly population. A substantial majority of patients with these fractures are over the age of 50, and cases occur among women 2–3 times more frequently than among men [4]. For these reasons, it is beneficial to conduct stress-deformation analyses and to assess the suitability of femoral nails for clinical treatment. The nails currently in use differ primarily in their design (collo-diaphyseal angle 120–135°, see Figure 1a) and also depending on the producer and the materials used (compatibility with the human body).

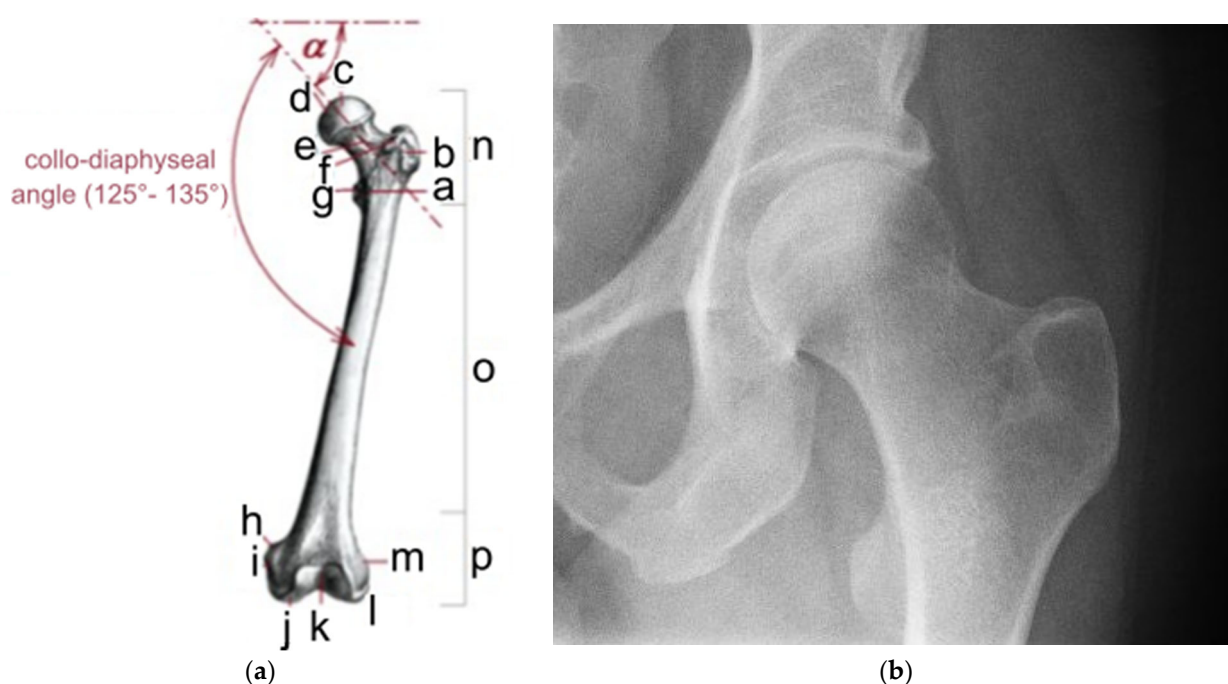


**Figure 1.** (a) Anatomy of femur bone (a—linea intertrochanterica; b—trochanter major; c—caput femoris; d—fovea capitis femoris; e—collum femoris; f—tuberositas glutea; g—trochanter minor; h—tuberculum adductorium; i—epicondylus medialis; j—condylus medialis; k—facies patellaris; l—condylus lateralis; m—epicondylus lateralis; n—proximal end; o—diaphysis; p—distal end). (b) Proximal femur placed in acetabulum (X-ray snapshot).

The femur (see Figure 1) is the largest and heaviest bone in the human body. The proximal part of the femur consists mainly of the almost spherical femoral head (caput femoris), which is seated within the acetabulum of the pelvis; the femoral neck (collum femoris), which forms the neck-shaft angle (collo-diaphyseal angle) with the main axial length of the femur (usually 125–135°); and the eminences of the greater and lesser trochanter (trochanter major and trochanter minor) and the adjacent areas, where the muscle attachments are located [1]. The anteversion of the femoral neck to the frontal anatomical plane is approximately 15°.

Proximal femoral fracture (PFF) is one of the most common types of long bone fracture and it presents a particular risk to elderly patients. We know that PFFs account for a large proportion of hospitalisations and possible complications among trauma cases [2].

More precise classifications of these fractures have been developed, facilitating practical description and enabling different treatment centres to share their clinical experiences. Historically, one of the best-known classifications of trochanteric fractures was developed by Evans [5], who divides them primarily into stable and unstable fractures and into several types. Figure 2a shows a classification of a fracture based on this system compared with the equivalent AO classification.

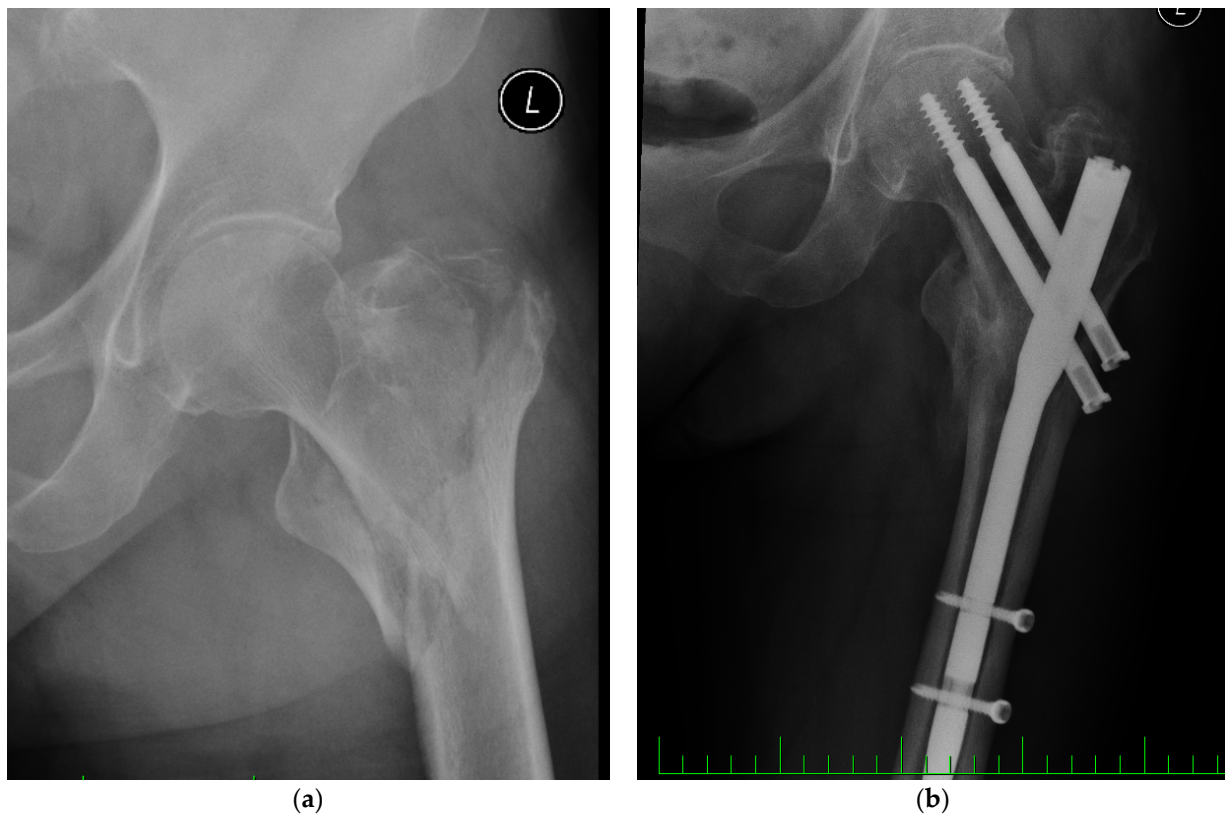


**Figure 2.** (a) Pertrochanteric fracture of femur (Evans 5, AO 31 A2.3); (b) fracture treatment via nail.

Femoral neck fractures have been described by numerous authors. One of the most frequently used classifications is by Garden [6], who divides fractures into four grades: I. incomplete, II. complete but non-displaced, III. complete and partially displaced and IV. complete and fully displaced.

Another classification of PFFs (and other fractures) is the international AO/OTA system, developed by the Swiss AO (Arbeitsgemeinschaft für Osteosynthesefragen) and the OTA (Orthopedic Trauma Association). This system uses numbers and letters to designate fracture types. PFFs are denoted by numbers from 31 upwards [3].

Each of these types of proximal femoral fracture requires special methods of treatment, each type has its own specific set of possible complications and controversies regarding optimal management methods. For more information on the various issues involved in the appropriate management of PFFs, please read the following [1,2,4].

PFFs among elderly people are mainly caused by simple falls. In younger patients, PFFs are most frequently caused by high-energy injuries, usually sustained due to traffic accidents, falls from heights, sporting injuries or occupational injuries.

Nowadays, such fractures are almost always treated surgically (osteosynthesis, alloplasty); exceptions are in cases when patients have contraindications to general or regional anaesthesia. The text below focuses mainly on osteosynthesis.

Surgery involves the repositioning and subsequent osteosynthesis of the broken bone, with metal implants used to fix the fractured parts of the bone in place; these may be either external or internal fixators [7,8]. As surgical methods have evolved, so too have the implants used for osteosynthesis in proximal femoral fractures [9]. In the past, plates with load screws were used [10]. Nowadays, osteosynthesis is usually achieved by using nails with several load screws [11]. The reliability of osteosynthesis depends on a number of factors, including the quality of the bone tissue (and its porosity or other degradation), the character of the fracture and the properties and shape of the implant used. The healing of the fracture is also affected by other factors, such as the patient's overall physical and

mental state, the condition of the soft tissue, the hormonal stability of the organism, possible infections, etc.

The choice of an appropriate implant, its properties and its shape have a substantial influence on the possible emergence of early and later postoperative complications, as well as on the duration of the healing process.

In this article, there are ten solved cases (i.e., ten numerical simulations) of fractured and healed femur with femoral nail implants with variability in collo-diaphyseal angles. Finite element method (FEM) was used to assess the suitability and reliability of all examined implants. FEM is widely used and accepted numerical method for solution of problems in mechanics and biomechanics. Quite a good review of FEM approach applied in lower limbs biomechanics can be seen in [12]. Similar numerical simulations were presented in reference [13].

## 2. Materials and Methods

Figure 3 briefly describes the process behind Materials and Methods chapter in pictures and is further explained in the following text below.

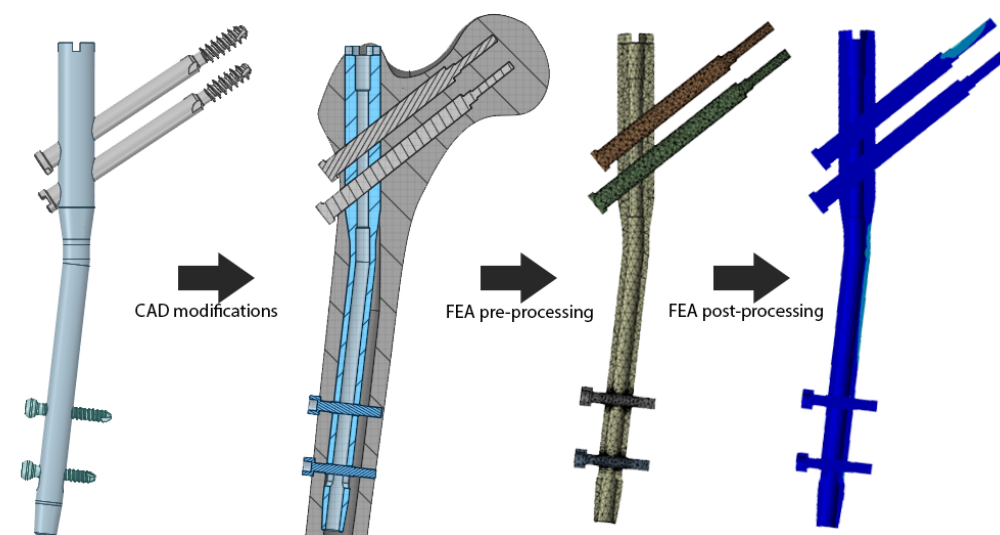


**Figure 3.** Workflow diagram.

The mechanical properties of the bone are considered to be isotropic and homogeneous; they are identical in all cases for the purposes of FEM analysis. All parts of the nails are produced from 1.4441 steel, which is commonly used in implants and is biocompatible [14–16]. Mechanical properties are shown in Table 1.

**Table 1.** Mechanical properties of materials used.

Material	Modulus of Tensile Elasticity/MPa/	Poisson's Constant/1/	Offset Yield Strength Rp0.2/MPa/	Tensile Strength Rm/MPa/
Bone	13,000	0.3	-	-
1.4441 steel	200,000	0.29	800	1000

The collo-diaphyseal angle of the anatomical model of the femur (Figures 1a and 4) obtained from a CT image is 125° [17]. The collo-diaphyseal angles of the investigated nails with variants of the femur are shown in Table 2. This variability was discussed with medics.

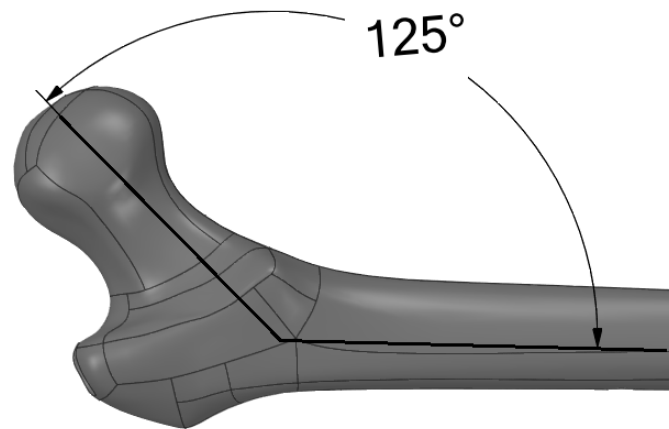


**Figure 4.** Collo-diaphyseal angle of anatomical CAD femur.

Note the difference between the collo-diaphyseal angle of the femur (which is a constant 125°) and the collo-diaphyseal angles of the nails (ranging from 120° to 135°) [18,19]. According to the anatomy of a patient, the manufacturer can produce implants with various collo-diaphyseal angles. Other dimensions may also vary depending on the patient’s anatomy, from which some are depicted in Figure 5.

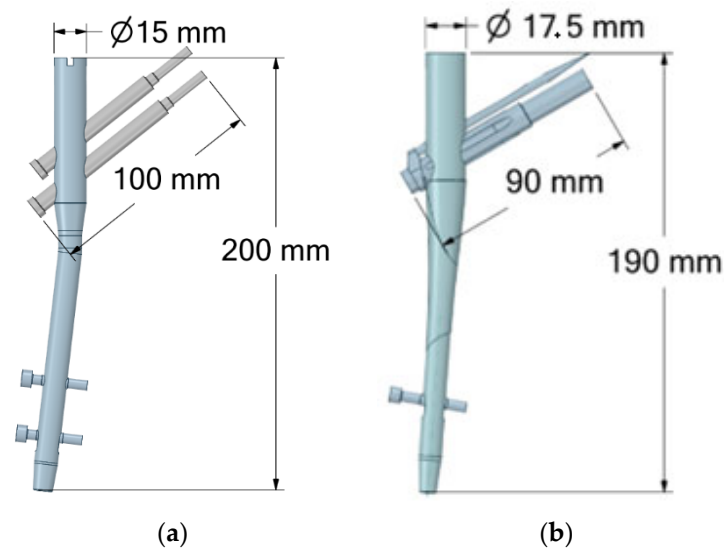


**Figure 5.** General dimensions of examined implants. (a) Medin; (b) Tantum.

**Table 2.** Cannulated nails under investigation.

Medin a.s.	Nail collo-diaphyseal angle 125°	Healed femur	Figure 6a
		Broken femur	Figure 7a
	Nail collo-diaphyseal angle 130°	Healed femur	Figure 6b
		Broken femur	Figure 7b
Tantum	Nail collo-diaphyseal angle 125°	Healed femur	Figure 6d
		Broken femur	Figure 7d
Tantum	Nail collo-diaphyseal angle 135°	Healed femur	Figure 6c
		Broken femur	Figure 7c
Tantum	Nail collo-diaphyseal angle 120°	Healed femur	Figure 6e
		Broken femur	Figure 7e

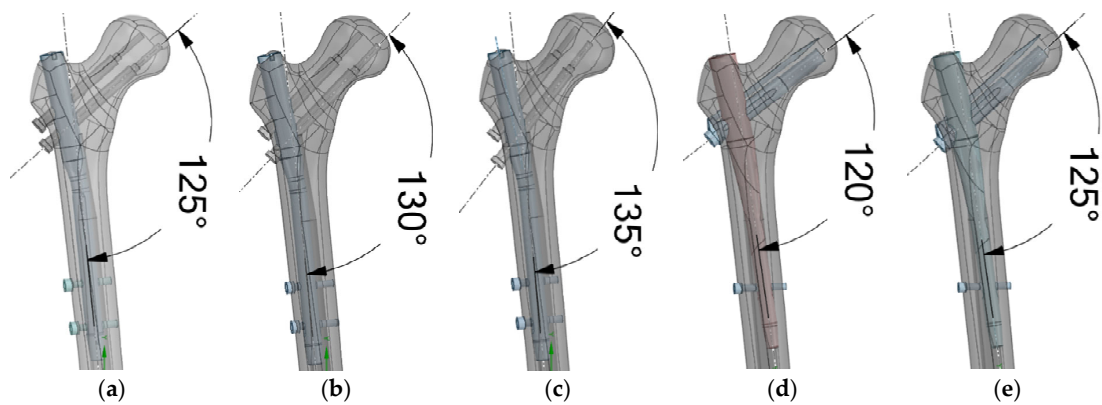


Figure 6. Modified CAD models of a healed femur with nails—(a–c) Medin; (d,e) Tantum.

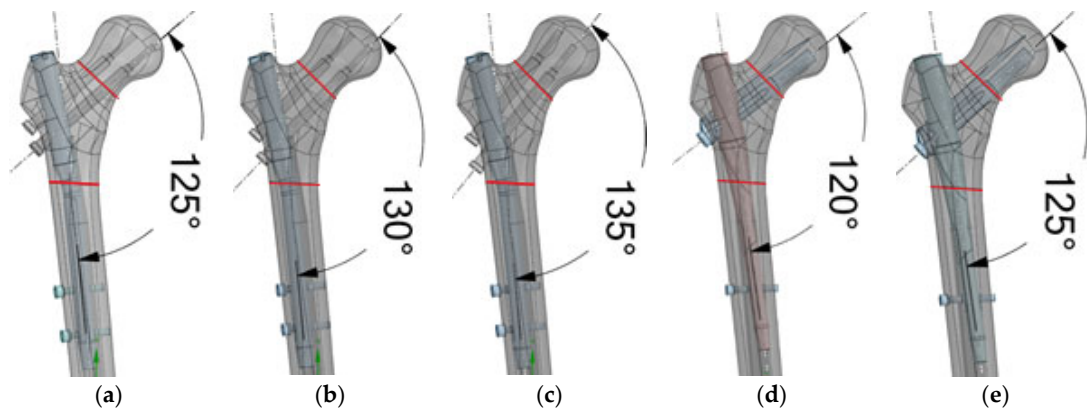


Figure 7. Modified CAD models of a broken femur with nails—(a–c) Medin; (d,e) Tantum.

In order to attain an acceptable level of simplification in the FEM simulation, the CAD models were modified appropriately (see Figure 8). This reduces computing time but has no substantial impact on the analytical results. The screws were modelled as pin-type structures; the screw thread was replaced by a cylindrical portion with the same diameter as the minor thread diameter (on the side of safety). The threads of the fixation screws were modified to approximately the mean diameter of the screw threads (representing an acceptable simplification), except at the point of contact with the nail, where the major thread diameter was retained (for accurate representation of the contact). The screw heads were modified to cylindrical volumes in order to simplify the simulation (this does not affect the results).

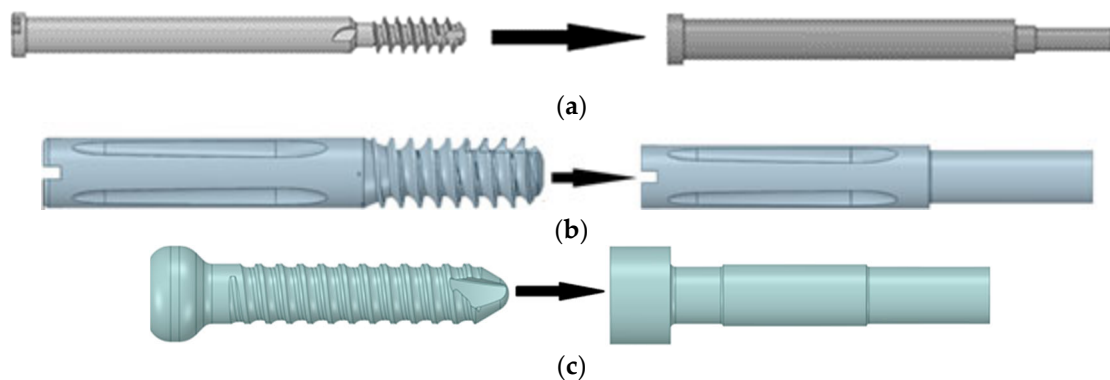
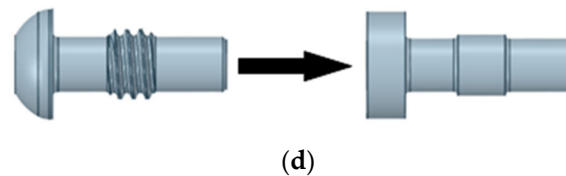
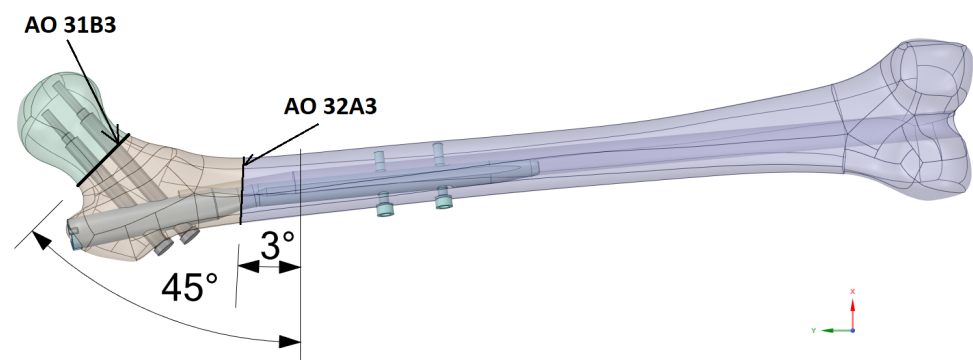


Figure 8. Cont.



**Figure 8.** Modifications of CAD models for FEM analysis. (a) Medin load screw; (b) Tantum load screw; (c,d) Fixation screws.

In the FEM analysis, fractures AO 31B1 and AO 32A3 (indicated in the preceding text and depicted in Figure 7) were created in the CAD model of the femoral bone by dividing the bone model along two planes, as indicated in Figure 9. Doctors from the University Hospital in Ostrava were consulted regarding the location of this division and approved the division.



**Figure 9.** Location of fractures in the anatomical CAD model of the femur (Spaceclaim).

### 3. Finite Element Analysis

The FEM analysis was conducted using Ansys Workbench 2020 R2 software [20].

Contacts were defined for the purpose of simulating mechanical contacts in all investigated models (see Figures 6 and 7). In principle, the contacts are the same in all the analyses, though there are differences between the healed and broken femurs, in the latter type there is also contact between the bone fragments (on the fracture surfaces). The contacts are shown in Table 3.

**Table 3.** Contacts (Ansys Workbench Mechanical software).

	Element	Femur	Screw
Healed femur	Femur	(One body)	Bonded
	Nail	Bonded	Bonded
Broken femur	Femur	Frictionless	Bonded
	Nail	Bonded	No separation

For the healed femur, it was considered that bone tissue has grown around all parts of the screws and nails, which means that neither the nail as a whole nor any part of it moves within the femur, so the nail can be considered a part of the bone. For this reason, the contacts were defined as “Bonded”.

For the broken femur, the contact types were chosen in order to simulate a situation in which the patient begins to place weight on the affected limb. In normal circumstances, weight-bearing begins 6 weeks after the implant is fitted and the patient should place no more than one-third of their total body weight on the healing limb. (Information gained from consultation with doctors) In some cases, the bone may suffer renewed damage at the location of the fracture, as it has not yet completely healed. In such cases there is no

displacement of the bone fragments, though the fragments may move slightly against each other.

For this reason, the contact was defined as “Frictionless”; this enables both tangential and normal displacement (separation). The contact is without a coefficient of friction, as the coefficient of friction between bones is not known. Moreover, in this case it is not necessary, as the entire movement of the bone is represented by the nail and its parts.

Because this is a simulation of the state of the femur after 6 weeks of treatment, it is considered that the bone tissue has already grown around all the recesses on the nails and their parts; the contact is thus defined as “Bonded”. For load screws and fixation screws, this contact would be provided by means of self-tapping screws during the initial implantation process.

Other boundary conditions used in the FEM analyses are shown in Figure 10. The hip joint region is subjected to compressive force  $F$  (C) and this is also the location of a contact permitting displacement only in the direction of the force application (B). Force  $F$  replaces the transfer of the patient’s weight—in this case a patient standing on one leg (extreme condition). For the purposes of the analysis, this force is considered to be static load with value of 1 N, and the necessary calculations are also carried out for other loading. In the knee joint region there is a boundary condition with a Winkler elastic foundation (D) with stiffness  $k = 0.13 \text{ N/mm}^3$  simulating the compressibility of joints (the reduction in the size of the spaces between the joints under loading) and a boundary condition only permitting displacement in the direction of the force application (A). Experiences of using elastic foundations were drawn from previous studies [1,2].

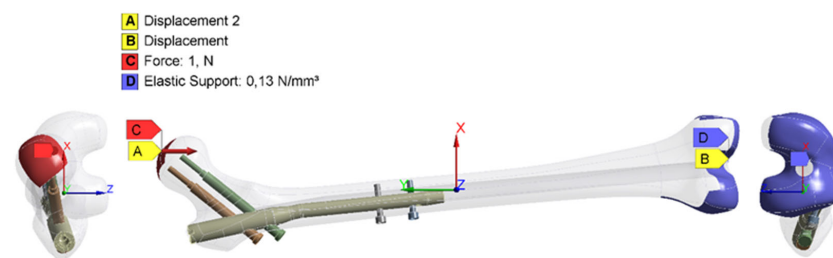


**Figure 10.** Boundary conditions.

The main element used in creating the finite element mesh was a ten-node quadratic tetrahedral element with three degrees of freedom in axes  $X$ ,  $Y$ ,  $Z$  in every node (solid 187, Ansys software [20]). This element is suitable for the meshing of irregular shapes, which is beneficial in this case. The mesh also used local refinement in the regions of contact and the regions of expected stress concentration. This initial mesh is shown for a Medin 125° cannulated nail in Figure 11, with details of the mesh refinement shown in Figure 12. The mesh properties for the individual systems are shown in Table 4.

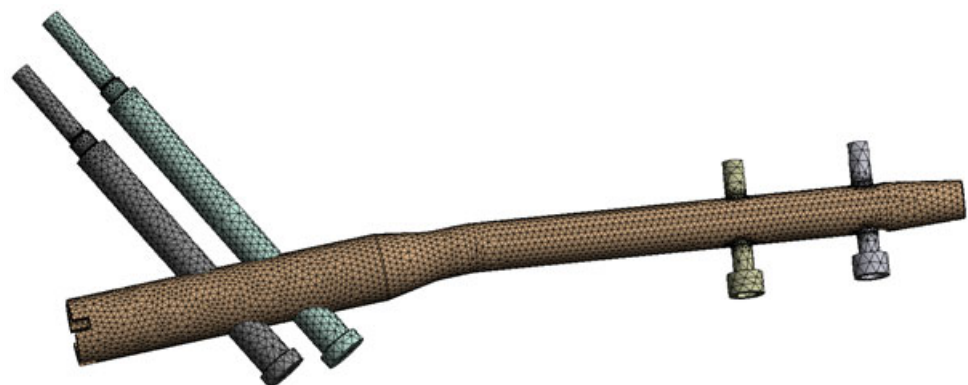


**Figure 11.** Finite element mesh for a Medin 125° nail.



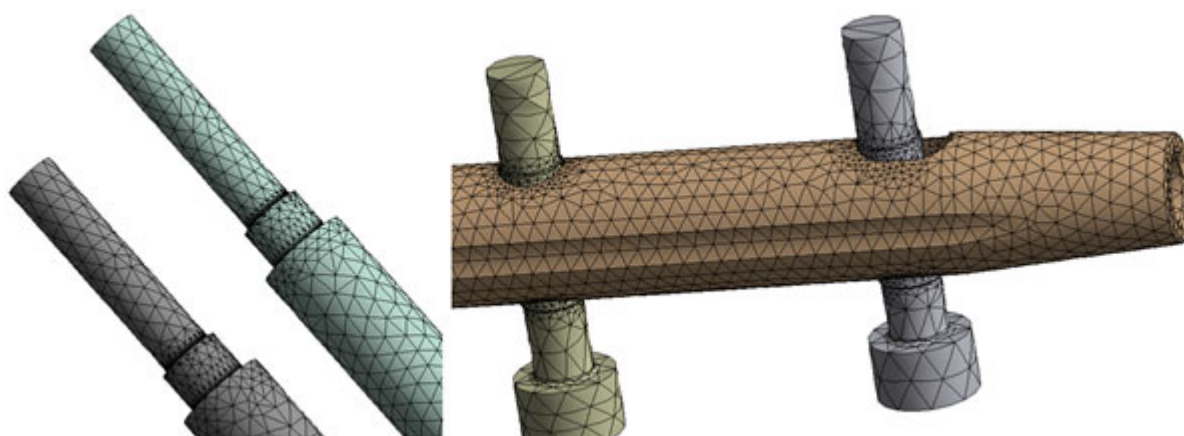


Figure 12. Local mesh refinement for a Medin 125° nail.

Table 4. Mesh properties.

			Σ of Elements	Σ of Nodes
Medin a.s.	Nail collo-diaphyseal angle 125°	Healed femur	111,447	188,515
		Broken femur	114,990	193,606
	Nail collo-diaphyseal angle 130°	Healed femur	101,685	172,160
		Broken femur	103,090	174,794
	Nail collo-diaphyseal angle 135°	Healed femur	102,524	173,702
		Broken femur	104,092	176,498
Tantum	Nail collo-diaphyseal angle 120°	Healed femur	113,942	190,439
		Broken femur	109,578	183,865
	Nail collo-diaphyseal angle 125°	Healed femur	110,558	185,967
		Broken femur	110,746	186,860

#### 4. Results

The values shown in Table 5 express the evaluated and maximum values of HMMH stress in MPa (occurring at the locations with stress concentrators, i.e., notches). The equivalent HMMH stress is generally determined by means of Equation (1). Extreme stress values occur locally in very small areas. The analysis also takes into account the so-called evaluated stress values occurring in the vicinity of the maximum (see Figure 13). Generally, the stresses occurring in the nail systems are considerably lower.

$$\sigma_{HMMH} = \sqrt{\sigma_1^2 + \sigma_2^2 + \sigma_3^2 - (\sigma_1\sigma_2 + \sigma_2\sigma_3 + \sigma_1\sigma_3)}, \tag{1}$$

where  $\sigma_i$  (MPa) are principle stresses.

Table 5. Stress values at F = 1 N results in 10<sup>-2</sup> MPa.

Nail Material	Femur	(HMMH) · 10 <sup>-2</sup> / MPa /	Medin			Tantum	
			125°	130°	135°	120°	125°
1.4441 steel	Healed femur	$\sigma_{ev} \div \sigma_{max}$	11.15 ÷ 12.55	5.69 ÷ 6.41	8.51 ÷ 9.58	7.46 ÷ 8.40	8.18 ÷ 9.21
	Broken femur	$\sigma_{ev} \div \sigma_{max}$	7.22 ÷ 8.12	5.58 ÷ 6.28	9.84 ÷ 11.07	5.45 ÷ 6.13	8.56 ÷ 9.63

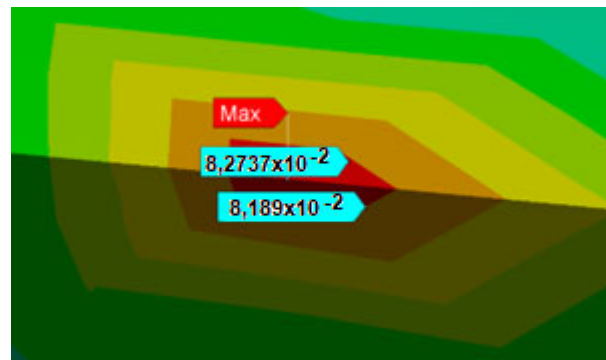


Figure 13. Example of maximum and evaluated HMH stress (MPa) (Tantum 125° healed femur).

Figures 14 and 15 show the HMH stress distribution caused by the action of force  $F = 1\text{ N}$  in the nail systems.

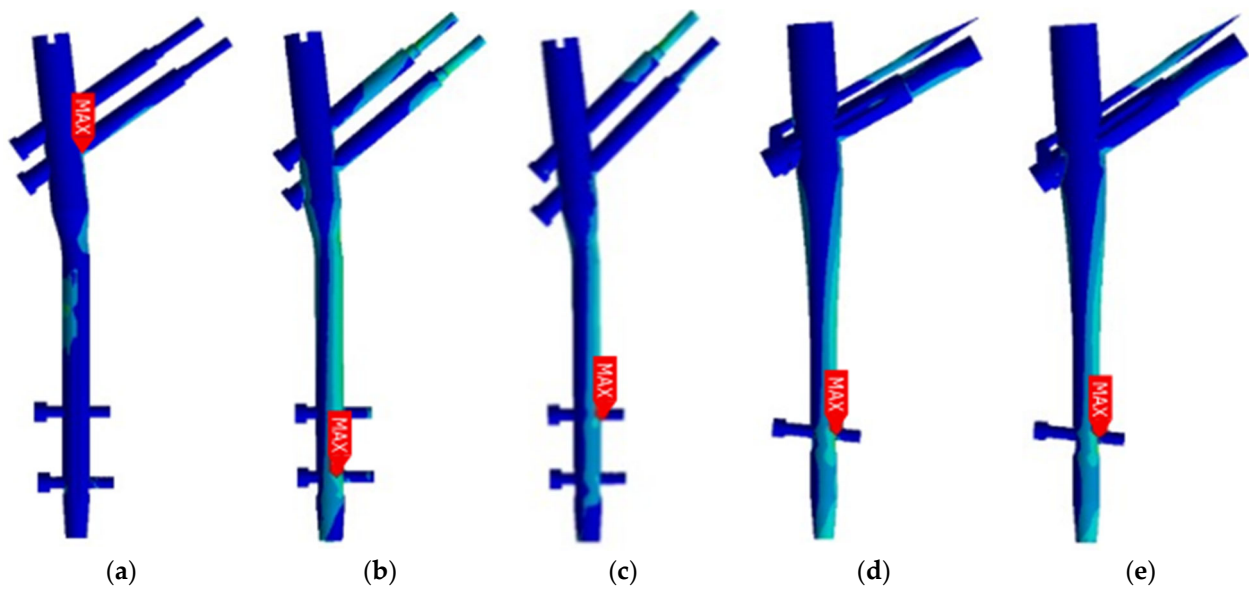


Figure 14. Stress distribution in the nail in the healed femur—(a–c) Medin and (d,e) Tantum. The image corresponds with Figure 6.

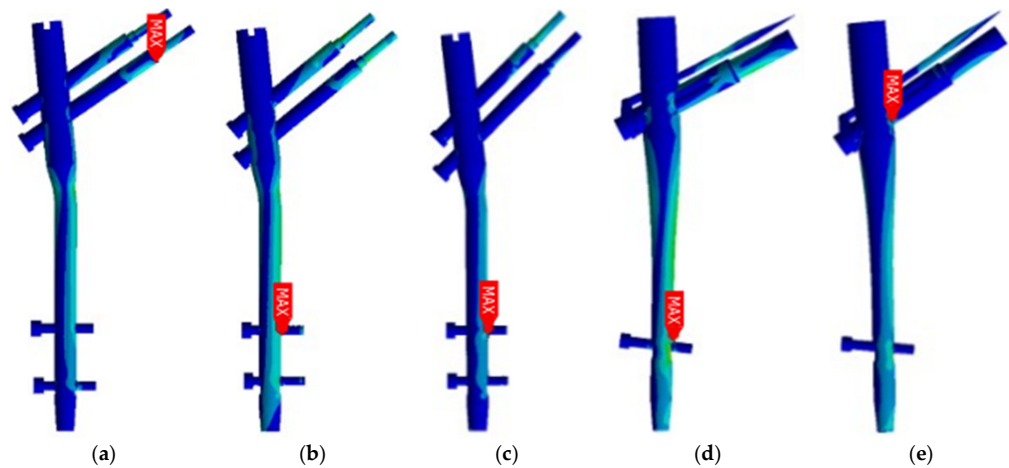


Figure 15. Stress distribution in the nail in the broken femur—(a–c) Medin and (d,e) Tantum. The image corresponds with Figure 7.

From the values shown in Table 5 (stress from loading with unit force), it is possible to use the linear dependence of stress on force to calculate stress under different forces. This is used when considering gravitational acceleration  $g = 9.807 \text{ ms}^{-2}$  and loading with force of equivalent mass  $m = 100 \text{ kg}$  (overloading of a single limb when standing on one foot). The calculation was carried out by means of Equations (2) and (3), and the resulting values are shown in Table 6. Examples of these calculations are given for the maximum stress for Medin 125° in a healed femur.

$$\sigma_{\max 100} = \sigma_{\max} \cdot m \cdot g \tag{2}$$

$$\sigma_{\max 100} = 12.55 \times 10^{-2} \times 100 \times 9.807 = 123.08 \text{ MPa} \tag{3}$$

**Table 6.** Stress values at  $F = 980.7 \text{ N}$ .

Nail Material	Femur	(HMH) /MPa/	Medin			Tantum	
			125°	130°	135°	120°	125°
1.4441 steel	Healed femur	$\sigma_{ev100} \div \sigma_{max100}$	109.35 ÷ 123.08	55.80 ÷ 62.86	83.46 ÷ 93.95	73.16 ÷ 82.38	80.22 ÷ 90.32
	Broken femur	$\sigma_{ev100} \div \sigma_{max100}$	70.81 ÷ 79.63	54.72 ÷ 61.59	96.50 ÷ 108.56	53.45 ÷ 60.12	83.95 ÷ 94.44

From the values given in Table 6, Equations (4) and (5) were used to determine the safety coefficient for the elasticity limit state, considering the offset yield strength  $R_{p0.2} = 800 \text{ MPa}$ —see Table 1. The safety values are given in Table 7.

$$k = \frac{R_{p0.2}}{\sigma_{\max 100}} \tag{4}$$

$$k = \frac{800}{123.08} = 6.5 \tag{5}$$

**Table 7.** Safety coefficients.

Nail Material	Femur	Safety k/1/	Medin			Tantum	
			125°	130°	135°	120°	125°
1.4441 steel	Healed femur	$k_{ev100}$	7.32	14.34	9.59	10.93	9.97
		$k_{max100}$	6.50	12.73	8.52	9.71	8.86
	Broken femur	$k_{ev100}$	11.30	14.62	8.29	14.97	9.53
		$k_{max100}$	10.05	12.99	7.37	13.31	8.47

Considering the extreme values, we are operating on the side of safety; the determined stress is far below the material yield strength—see Table 1. Considering the safety coefficients shown in Table 7, we can state that these coefficients are sufficiently high, even when considering maximum values occurring at the notch points (extreme values for the side of safety). It can therefore be stated that all the nails investigated in this study are sufficiently safe and reliable.

Limitations of our results are based on examined materials, specific types of implants and our quasistatic approach, i.e., negligence of dynamical effects. Mentioned dynamical effects can be neglected because the patient must stay in bed for a “short” time after surgery, which is examined case by case.

Similar studies examining femoral nails and dynamic hip screws are presented in [21–23]. In these references, the results are acquired via numerical approaches and experiments. Similar to our results, the implants are suitable for clinical use.

### 5. Discussion

Initial FEM calculations were carried out, enabling the comparison of proximal femoral nails made by two manufacturers, Medin and Tantum [18,19]. The results, i.e., the safety of nails (Table 7), are satisfactory and the nails are appropriate for normal medical use.

Figures 16–19 below depict the values of the maximum and evaluated HMH stresses (MPa) depending on the collo-diaphyseal angle of the nail in healed and broken femurs. The values of these stresses correspond with the loading of force  $F = 980.7 \text{ N}$ .

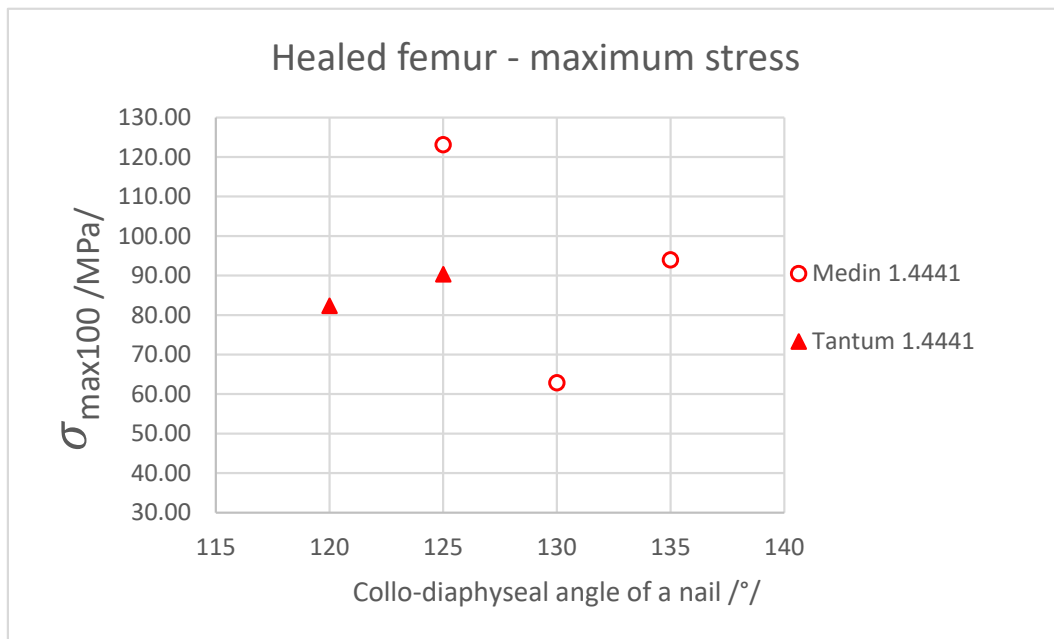


Figure 16. Dependence of maximum HMH stress (MPa) on nail collo-diaphyseal angle (healed femur).

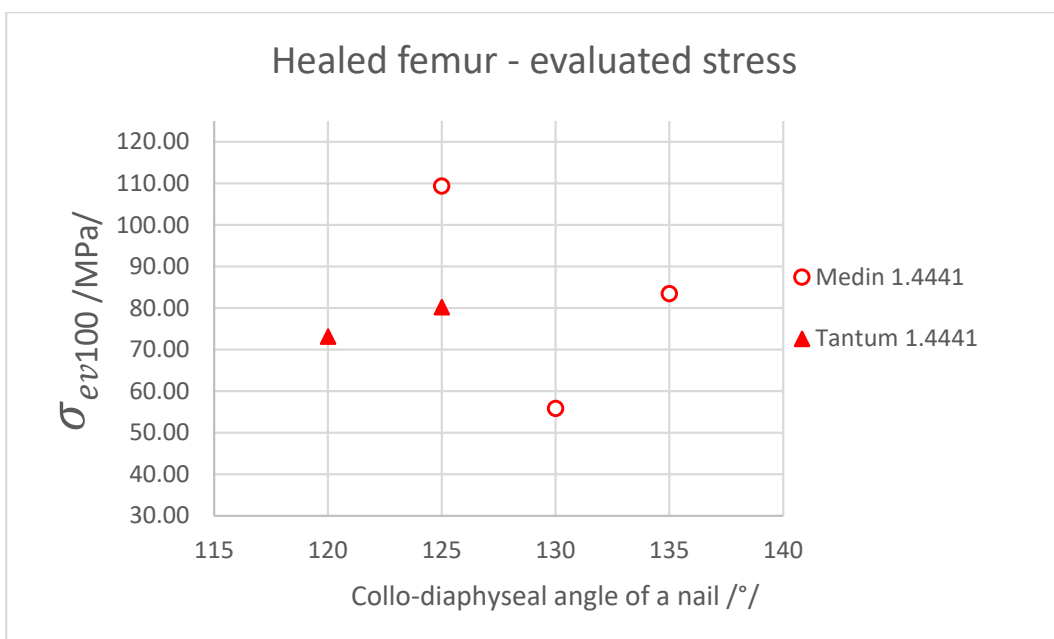
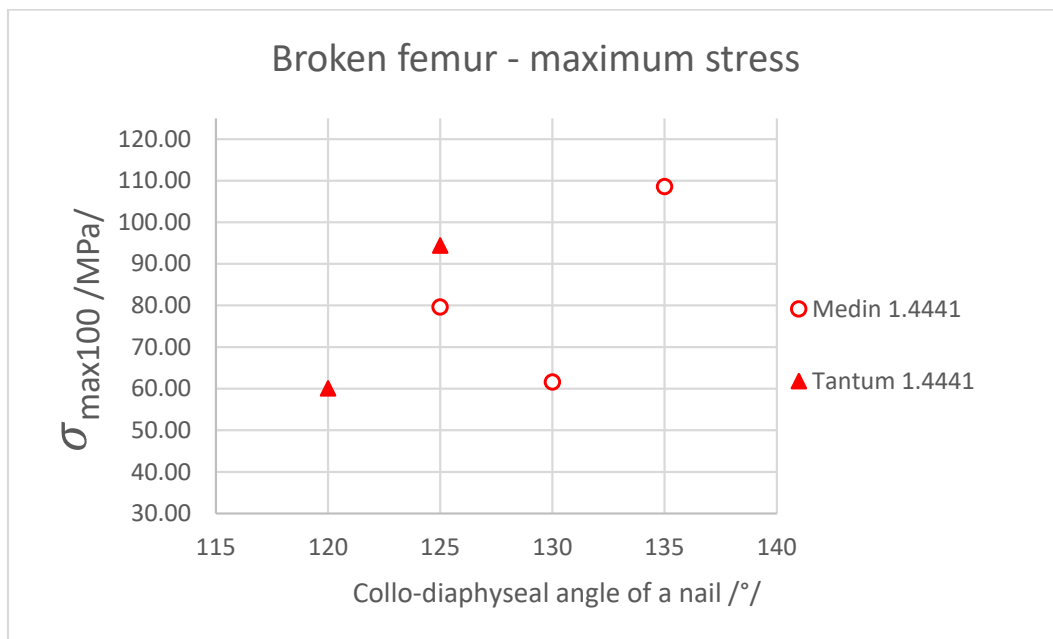
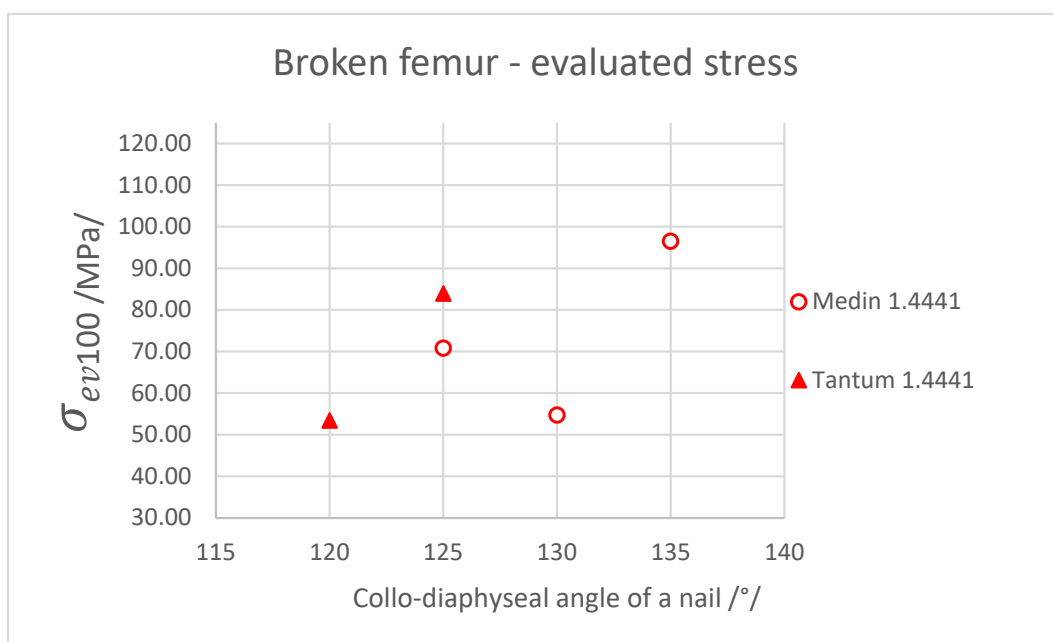


Figure 17. Dependence of evaluated HMH stress (MPa) on nail collo-diaphyseal angle (healed femur).



**Figure 18.** Dependence of maximum HMH stress (MPa) on nail collo-diaphyseal angle (broken femur).



**Figure 19.** Dependence of evaluated HMH stress (MPa) on nail collo-diaphyseal angle (broken femur).

From Tables 5–7 and Figures 16–19 it is possible to determine which implants (femoral nails) are most appropriate for use in treatment. No correlation was found between the collo-diaphyseal angle of the nails and HMH stress.

The factor for determining the most suitable implant is the lowest value of maximum and evaluated HMH stress, which is associated with levels of safety. In this case, the safety level should be as high as possible.

Additional tasks which would be appropriate for the investigation of femoral nailing would primarily involve experiments on replica bones (whose mechanical properties would correspond with those of real bones) in combination with femoral nails subjected to compressive (or tensile) and bending load. These experiments can be performed similarly as in our previous work [24] and other experiments [25].

It would also be appropriate to follow up these experiments with numerical analysis in the form of FEM calculations, this would allow for comparison with the experimental results [1,26,27]. Stochastic (probabilistic) approaches are a viable option as well [2].

A further task would be to use a model of a bone created via reconstruction from a CT image; in this case, the material model used in the calculation would be close to reality. This would reveal non-homogeneity and anisotropy in the material and it would thus enable more precise FEM analyses to be carried out, yielding more accurate results [28].

A more accurate material model would also make it possible to carry out analyses of anatomic models of femurs with various collo-diaphyseal angles, for example via Mimics sw. [29]. If sufficiently precise material properties were used, it would be possible to investigate the dynamics and propagation of fractures in bones.

## 6. Conclusions

This article introduces anatomy, physiology and treatment of proximal femur fractures AO 31B3 and AO 32A3. Biomechanical assessments of ten cannulated nails produced by Medin a.s. and Tantum companies were performed. From the finite element analyses of femurs with cannulated nails with or without fractures, is evident that even for extreme stress values, the safety levels for the elasticity limit state are very high. Calculated stresses based on variable collo-diaphyseal angles of 120° to 135° give safety values ranging from 6.50 to 14.97. This indicates that the implants are suitable for use in patient treatment.

However, it is important to be aware that the real-life application of nails differs from patient to patient (due to the collo-diaphyseal angle of the femur, the material properties of the bone, etc.). These circumstances have a major influence on the transfer of force from the body (the bone) to the implant. As a consequence, each case is highly individual, so the values may differ substantially between patients.

However, even in cases when the stress values in the nail are different, this should not lead to a substantial reduction in the implant's safety at elasticity limit states. This indicates that the implants can be used in a wide range of situations and can thus be recommended for clinical use.

The comparison between the nails manufactured by Medin and those manufactured by Tantum shows that both types of nails are equally appropriate and sufficiently safe. The choice of nail and its application thus depend on other parameters of the human body.

**Author Contributions:** Conceptualization, K.F.; Project administration, L.P.; Resources, R.M., M.H., L.P. and P.K.; Writing—original draft, K.F., T.H., D.Č., O.S., K.D., A.T. and J.H.; Writing—review & editing, K.F., T.H., D.Č., V.M., K.D., K.Š. and Z.M. All authors have read and agreed to the published version of the manuscript.

**Funding:** Ministry of Education Youth and Sports—SP2021/66 “Use of experimental and computational modeling problems of elastic and flexible bodies”; European Union and Government of the Czech Republic—CZ.02.1.01/0.0/17\_049/0008407 “Innovative and additive manufacturing technology—new technological solutions for 3D printing of metals and composite materials”; European Union and Government of the Czech Republic—CZ.02.1.01/0.0/0.0/17\_049/0008441 “Innovative Therapeutic Methods of Musculoskeletal System in Accident Surgery”.

**Institutional Review Board Statement:** Not applicable.

**Informed Consent Statement:** Not applicable.

**Data Availability Statement:** Not applicable.

**Acknowledgments:** The research for this article was funded by the Czech project SP2021/66 and by the projects CZ.02.1.01/0.0/17\_049/0008407 and CZ.02.1.01/0.0/0.0/17\_049/0008441 within the Operational Programme Research, Development and Education financed by the European Union and from the state budget of the Czech Republic.

**Conflicts of Interest:** The authors declare no conflict of interest.

## References

1. Frydryšek, K.; Šír, M.; Pleva, L. Strength Analyses of Screws for Femoral Neck Fractures. *J. Med. Biol. Eng.* **2018**, *38*, 816–834. [CrossRef] [PubMed]
2. Frydryšek, K.; Šír, M.; Pleva, L.; Szeliga, J.; Stránský, J.; Čepica, D.; Kratochvíl, J.; Koutecký, J.; Madeja, R.; Dědková, K.P.; et al. Stochastic Strength Analyses of Screws for Femoral Neck Fractures. *Appl. Sci.* **2022**, *12*, 1015. [CrossRef]
3. Meinberg, E.; Agel, J.; Roberts, C.; Karam, M.D.; Kellam, J.F. Fracture and Dislocation Classification Compendium—2018. *J. Orthop. Trauma* **2018**, *32*, S1–S10. [CrossRef] [PubMed]
4. Mittal, R.; Banerjee, S. Proximal femoral fractures: Principles of management and review of literature. *J. Clin. Orthop. Trauma* **2012**, *3*, 15–23. [CrossRef]
5. Evans, E.M. The treatment of trochanteric fractures of the femur. *J. Bone Jt. Surg.* **1949**, *31*, 190–203. [CrossRef]
6. Garden, R.S. Low-Angle Fixation in Fractures of the Femoral Neck. *J. Bone Jt. Surgery. Br. Vol.* **1961**, *43*, 647–663. [CrossRef]
7. Theisz, G.; Frydryšek, K.; Fojtík, F.; Pečenka, L.; Kubín, T.; Sadilek, M.; Kratochvíl, J.; Demel, J.; Madeja, R.; Pleva, L. Locking Compression Plate for Distal Tibia Fractures. *Appl. Mech. Mater.* **2016**, *827*, 359–366. [CrossRef]
8. Frydryšek, K.; Theisz, G.; Bialy, L.; Pliska, L.; Pleva, L. Finite element modelling of T-plate for treatment of distal radius. In *Intelligent Systems for Computer Modelling. Advances in Intelligent Systems and Computing*; Stýskala, V., Kolosov, D., Snášel, V., Karakeyev, T., Abraham, A., Eds.; Springer: Cham, Switzerland, 2016; Volume 423. [CrossRef]
9. Bartoniček, J.; Rammelt, S. The history of internal fixation of proximal femur fractures Ernst Pohl—The genius behind. *Int. Orthop.* **2014**, *38*, 2421–2426. [CrossRef]
10. Hasenboehler, E.A.; Agudelo, J.F.; Morgan, S.J.; Smith, W.R.; Hak, D.J.; Stahel, P.F. Treatment of Complex Proximal Femoral Fractures with the Proximal Femur Locking Compression Plate. *Orthopedics* **2007**, *30*, 618–623.
11. Simmermacher, R.; Bosch, A.; Van der Werken, C. The AO/ASIF-proximal femoral nail (PFN): A new device for the treatment of unstable proximal femoral fractures. *Injury* **1999**, *30*, 327–332. [CrossRef]
12. Ramlee, M.H. Finite Element Modelling and Simulation for Lower Limb of Human Bone: A Review. *Mal. J. Med. Health Sci.* **2020**, *16*, 262–271.
13. Jamari, J.; Ammarullah, M.; Saad, A.; Syahrom, A.; Uddin, M.; van der Heide, E.; Basri, H. The Effect of Bottom Profile Dimples on the Femoral Head on Wear in Metal-on-Metal Total Hip Arthroplasty. *J. Funct. Biomater.* **2021**, *12*, 38. [CrossRef]
14. Čada, R.; Frydryšek, K.; Sejda, F.; Demel, J.; Pleva, L. Analysis of Locking Self-Taping Bone Screws for Angularly Stable Plates. *J. Med. Biol. Eng.* **2017**, *37*, 612–625. [CrossRef]
15. Drápala, J.; Kostiuková, G.; Losertová, M. Influence of heat treatment on microstructure and mechanical properties of SUS 316L alloy. In Proceedings of the 27th International Conference on Metallurgy and Materials (METAL), Brno, Czech Republic, 23–25 May 2018; pp. 1527–1532.
16. Hlinka, J.; Dostalova, K.; Dedkova, K.P.; Madeja, R.; Frydrysek, K.; Koutecky, J.; Sova, P.; Douglas, T.E.L. Complex Material and Surface Analysis of Anterolateral Distal Tibial Plate of 1.4441 Steel. *Metals* **2021**, *12*, 60. [CrossRef]
17. Deswal, A.; Saxena, A.K.; Bala, A. Measurement of Collo-Diaphyseal Angle and Femoral Neck Anteversion Angle of Femur Bone. *Int. J. Sci. Stud.* **2017**, *5*, 97–99.
18. MEDIN. *Instruments and Implants for Traumatology*; MEDIN: Nové Město na Moravě, Czech Republic, 2018; pp. E5.3–E5.4. Available online: [https://www.medin.cz/media/cache/file/ce/medin-traumatology-catalogue-2018-10-CS-EN\\_LQ.pdf](https://www.medin.cz/media/cache/file/ce/medin-traumatology-catalogue-2018-10-CS-EN_LQ.pdf) (accessed on 21 April 2022).
19. Tantum. Systemübersicht PLATON. Available online: [https://tantum-ag.de/wp-content/uploads/2018/09/b\\_02\\_11.1\\_platon\\_broschuere.pdf](https://tantum-ag.de/wp-content/uploads/2018/09/b_02_11.1_platon_broschuere.pdf) (accessed on 21 April 2022).
20. Ansys. Ansys Workbench 2020 R2. 2020. Available online: <https://www.ansys.com/products/ansys-workbench> (accessed on 21 April 2022).
21. Steinberg, E.L.; Blumberg, N.; Dekel, S. The fixation proximal femur nailing system: Biomechanical properties of the nail and a cadaveric study. *J. Biomech.* **2005**, *38*, 63–68. [CrossRef]
22. Moon, J.K.; Lee, J.I.; Hwang, K.T.; Yang, J.-H.; Park, Y.-S.; Park, K.-C. Biomechanical comparison of the femoral neck system and the dynamic hip screw in basicervical femoral neck fractures. *Sci. Rep.* **2022**, *12*, 7915. [CrossRef]
23. Huang, Y.; Zhang, C.; Luo, Y. A comparative biomechanical study of proximal femoral nail (InterTAN) and proximal femoral nail antirotation for intertrochanteric fractures. *Int. Orthop.* **2013**, *37*, 2465–2473. [CrossRef]
24. Frydryšek, K.; Čepica, D.; Halo, T.; Skoupý, O.; Pleva, L.; Madeja, R.; Pometlová, J.; Losertová, M.; Koutecký, J.; Michal, P.; et al. Biomechanical Analysis of Staples for Epiphysiodesis. *Appl. Sci.* **2022**, *12*, 614. [CrossRef]
25. Cristofolini, L.; Viceconti, M.; Cappello, A.; Toni, A. Mechanical validation of whole bone composite femur models. *J. Biomech.* **1996**, *29*, 525–535. [CrossRef]
26. Orwoll, E.S.; Marshall, L.M.; Nielson, C.M.; Cummings, S.R.; Lapidus, J.; Cauley, J.A.; Ensrud, K.; Lane, N.; Hoffmann, P.R.; Kopperdahl, D.L.; et al. Finite Element Analysis of the Proximal Femur and Hip Fracture Risk in Older Men. *J. Bone Miner. Res.* **2009**, *24*, 475–483. [CrossRef]
27. Grassi, L.; Väänänen, S.; Yavari, S.A.; Weinans, H.; Jurvelin, J.S.; Zadpoor, A.A.; Isaksson, H. Experimental validation of finite element model for proximal composite femur using optical measurements. *J. Mech. Behav. Biomed. Mater.* **2013**, *21*, 86–94. [CrossRef]

28. Nizamuddin, M.K.; Kirthana, S. Reconstruction of human femur bone from CT scan images using CAD techniques. *IOP Conf. Ser. Mater. Sci. Eng.* **2018**, *455*, 012103. [[CrossRef](#)]
29. Materialise. Mimics Innovation Suite. Medical Image Analysis Software. Available online: <https://www.materialise.com/en> (accessed on 21 April 2022).